Steps towards molecular parity violation in axially chiral molecules. I. Theory for allene and 1,3-difluoroallene

Michael Gottselig, and Martin Quack

View Online   Export Citation

ARTICLES YOU MAY BE INTERESTED IN

Infrared laser induced population transfer and parity selection in $^{14}NH_3$: A proof of principle experiment towards detecting parity violation in chiral molecules
The Journal of Chemical Physics **143**, 244305 (2015); https://doi.org/10.1063/1.4936912

Combined multidimensional anharmonic and parity violating effects in CDBrClF
The Journal of Chemical Physics **119**, 11228 (2003); https://doi.org/10.1063/1.1622381

Theory of a two-step enantiomeric purification of racemic mixtures by optical means: The D_2S_2 molecule
The Journal of Chemical Physics **119**, 5105 (2003); https://doi.org/10.1063/1.1597491

AIP Publishing

Steps towards molecular parity violation in axially chiral molecules. I. Theory for allene and 1,3-difluoroallene

Michael Gottselig and Martin Quack[a)]
Physical Chemistry, Eidgenössische Technische Hochschule (ETH) Zurich, CH-8093 Zurich, Switzerland

In view of exploring possibilities for an experimental investigation of molecular parity violation we report quantum-chemical calculations of the parity-conserving and parity-violating potentials in the framework of electroweak quantum chemistry in allene C_3H_4 and 1,3-difluoroallene $C_3H_2F_2$, which is nonplanar and axially chiral in the electronic ground state but expected to be nearly planar and achiral in several electronically excited states. The parity-violating potentials E_{pv} for allene and 1,3-difluoroallene calculated with the multiconfiguration linear-response (MC-LR) approach of Berger and Quack [J. Chem. Phys. **112**, 3148 (2000)] show qualitatively similar behavior as a function of torsional angle τ with maximum values of about 0.5 pJ mol^{-1} for C_3H_4 and 2 pJ mol^{-1} for $C_3H_2F_2$. However, in the latter case they are asymmetrically shifted around $\tau=90°$, with a nonzero value at the chiral equilibrium geometry resulting in a parity-violating energy difference between enantiomers $\Delta_{pv}E=E_{pv}(P)-E_{pv}(M)=1.2$ pJ mol^{-1} (equivalent to about 10^{-13} cm^{-1}). The calculated barrier heights corresponding to the nonrigid (multiple, and in part chiral) transition states in 1,3-difluoroallene fall in the range of 180–200 kJ mol^{-1}. These high barriers result in hypothetical tunneling splittings much smaller than $\Delta_{pv}E$ and thus parity violation dominates over tunneling for the stereomutation dynamics in 1,3-difluoroallene. Therefore, $\Delta_{pv}E$ is predicted to be a spectroscopically measurable energy difference. Two of the lower excited electronic states of $C_3H_2F_2$ (^1A and ^3A) are calculated to be planar or quasiplanar, allowing, in principle, for spectroscopic state selection of states of well-defined parity. The results are discussed in relation to possible schemes of measuring parity violation in chiral molecules. © *2005 American Institute of Physics.* [DOI: 10.1063/1.1884114]

I. INTRODUCTION

Rather soon after the discovery of parity violation in nuclear physics[1–3] speculations about the role of molecular parity violation appeared, particularly in relation to the origin of biomolecular homochirality.[4–6] The first quantitative theoretical calculations of the very small effects of molecular parity violation appeared more than 20 years ago,[7] but the more recent finding that effective parity-violating potentials calculated by new theoretical approaches are typically one to two orders of magnitude larger than previously anticipated has provided new impetus to the field[8–13] (see also the recent review[6]). However, experimental approaches towards molecular parity violation are rather limited and so far unsuccessful.[6,14–25]

Apart from possible macroscopic phenomena in condensed phases, which we shall not discuss here, as they are unlikely to yield quantitative proof and measurements comparable to theoretical predictions,[6,26] one can distinguish basically three conceptually different experimental approaches to molecular parity violation that are based on gas phase molecular spectroscopy. In the first approach, proposed by Letokhov and co-workers in 1975–1976,[15] one tries to measure frequency shifts $\Delta\nu=\nu_R-\nu_S$ between corresponding pairs of high-resolution spectral lines in the two enantiomers

(R and S) of a chiral molecule. Several experimental tests related to such shifts have been made in the infrared and microwave ranges,[16,22–24] but in agreement with the calculated relative frequency shift $\Delta\nu/\nu$ being very small (about 10^{-16} for not too heavy elements[14,27–29]), none of them was successful. The same is true for the more difficult to interpret shifts in condensed phase NMR and Mössbauer spectra.[19–21,29]

A second proposal relies on the measurement of time-dependent optical activity in chiral molecules, which have the special property that tunneling splittings are of the same order of magnitude as the parity-violating potentials.[17] Meanwhile, quantitative calculations on tunneling and parity violation have identified a few examples of such molecules,[30–33] but to our knowledge there is currently no serious experimental effort under way along these lines.

A third proposed scheme for experiments on parity violation has the particular advantage that it provides in principle a measurement of the parity-violating energy difference $\Delta_{pv}E$ between enantiomers in their ground states, related to the enthalpy $\Delta_{pv}H_0^{\Theta}$ of enantiomerization

$$R \rightleftarrows S, \quad \Delta_{pv}H_0^{\Theta} = N_A\Delta_{pv}E. \tag{1}$$

This scheme uses resolved spectroscopic intermediate states that are achiral, and thus needs high rovibrational line resolution.[18,25] As outlined in Fig. 1, this approach can provide $\Delta_{pv}E$ by combination difference of two allowed spectral

a)Author to whom correspondence should be addressed. Fax: ++41 1 632 10 21. Electronic mail: martin@quack.ch
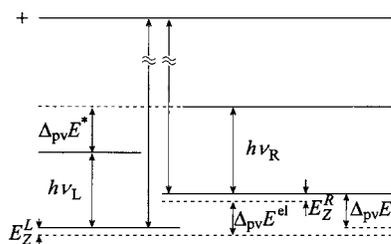
FIG. 1. Energy-level diagram for "left" (L) and "right" (R) enantiomers of a chiral molecule modified from Ref. 28. Microscopic experimental (spectroscopic) schemes aim to measure a parity-violating frequency shift, that is, a difference in spectral transitions $h\nu_L$ and $h\nu_R$ in the separate enantiomers (the spectral transitions can principally be in the NMR, microwave, IR, UV/Vis, or γ-ray range). The measurement of such a parity-violating frequency shift would correspond to the determination of differences $|\Delta_{pv}E^* - \Delta_{pv}E|$ of parity-violating differences and would not allow the determination of the very interesting parity-violating energy difference $\Delta_{pv}E$ itself. Experimental approaches that would allow the measurement of the latter quantity make use of spectral transitions to an achiral excited (vibrational or electronic) state with well-defined parity (here positive +; see spectral transitions in the middle). This approach can be realized with time-independent and time-dependent spectroscopic approaches (see Refs. 6 and 25). The long-dashed lines indicate the electronic potential-energy minima including parity-violating potentials, whereas the solid lines indicate vibrational (ground and excited state) levels including zero-point energy (E_Z) and parity-violating corrections (not to scale). The transitions (vertical lines) to the dashed lines are forbidden, whereas transitions between full lines are observable spectroscopically.

FIG. 2. The two enantiomers (left: P form; right: M form) of chiral 1,3-difluoroallene in a collinear C_2-symmetric geometry are shown, including the internal coordinates along which the ground-state potential-energy surface of 1,3-difluoroallene was calculated: τ is the torsional coordinate, α the in-plane and α' the out-of plane CCC-angle bending coordinates, whereby "in-plane" and "out-of-plane" refer to the planar structures at $\tau=0°$ and $\tau=180°$.

lines or else it can be carried out in a time-dependent fashion using nonclassical[34] superposition states of the two different R and S enantiomers, with initially well-defined parity, showing time evolution of parity due to parity violation.[18] An interesting class of molecules that are useful in such a scheme may be molecules that are nonplanar and chiral in their ground electronic states, but achiral, planar, or quasiplanar in some of their excited states. Allenes were suggested among other candidates for such molecules.[18] The basic molecular scheme of (Ref. 18) outlined in Fig. 1 can also be used to address other questions such as the superselection rule hypothesis,[34] testing the collision hypothesis of chirality and related questions,[25,35] designing ultrafast optical switches,[36] or separating enantiomers of chiral molecules with coherent control.[37,38] For more comprehensive reviews with a more complete survey of the literature, see Refs. 6, 25, and 27.

Numerous spectroscopic difficulties have to be overcome in realizing molecular experiments relating to the scheme of Fig. 1. The goal of the present work is to provide a theoretical and spectroscopic proof of principle that includes some of the high-resolution spectroscopic ground work and quantitative theoretical calculations on a real molecule, difluoroallene, which is a first example for which such detailed results are now becoming available. Difluoroallene (Fig. 2) was synthesized[39] in 1974 (see also Ref. 40) and there have been a few spectroscopic and theoretical investigations on this molecule within a "classical" (i.e., non-parity violating) context since that time.[41–45] In particular, the ^{13}C NMR spectrum was measured,[39] the microwave rotational spectrum was analyzed successfully,[41] and the infrared and Raman spectra recorded at modest resolution,[42] leading to a tentative normal-mode assignment.

The present work is divided into two parts. In a first paper we present theoretical calculations on parity-conserving and parity-violating potentials in allene and difluoroallene, providing also quantitative evidence for the existence of the achiral excited state necessary for the realization of the experimental scheme outlined above. In a second paper we present a first high-resolution rovibrational analysis of a part of the infrared spectrum, which is a necessary first step for the rovibrational state and parity selection in such experiments (see Ref. 46).

The calculations presented here for the unsubstituted allene should be seen mostly as a starting point for 1,3-difluoroallene. Although 1,3-dideuteroallene has been discussed in relation to parity violation as well,[25] the expected effects are smaller than with fluorine substitution. There has been a substantial amount of work on ground- and excited-state potentials for allene, which provides a background for our calculations.[47–57]

II. THEORETICAL METHODS AND COMPUTATIONAL DETAILS

A. Electronic ground states

Geometry optimizations in the electronic ground state along the torsional coordinate τ for allene and along the torsional, in-plane α and out-of-plane α' CCC-angle bending coordinates for 1,3-difluoroallene were performed with GAUSSIAN 98 (Ref. 58) using the complete active space self-consistent-field (CASSCF) method (note that "in-plane" and "out-of-plane" refer to the planar structures at $\tau=0°$ and $\tau=180°$, see Fig. 2). All geometry optimizations used Gaussian's "tight" optimization criterion. The torsional potential-energy surface of allene is symmetric with respect to the equilibrium structure ($\tau=90°$). Thus, it is sufficient to perform all parity-conserving calculations within the range of $\tau=0°-90°$. The torsional potential-energy surface of 1,3-difluoroallene is symmetric with respect to the planar geometry at $\tau=180°$. Thus, we calculated the torsional potential within the range of $\tau=0°-180°$. For both molecules the calculations were performed in 10° steps along the torsional coordinate. The selection of the active space as well as the calculation of appropriate starting orbitals used Pulay and Hamilton's method.[59] Firstly, unrestricted Hartree–Fock (UHF) calculations were performed for rigidly twisted allene

and 1,3-difluoroallene using the correlation consistent polarized valence double zeta (cc-pVDZ) basis set. Starting structures for allene were derived from a previously reported equilibrium geometry,[56] and starting structures for 1,3-difluoroallene were derived from the minimum structure that was obtained in a preceding second-order Møller–Plesset/correlation consistent polarized valence triple zeta (MP2/cc-pVTZ) geometry optimization within the constraints of C_2 symmetry and C–C–C collinearity. Secondly, for each geometry, natural orbitals of the UHF wave function were selected as starting orbitals for subsequent CASSCF calculations, whereby the inclusion of natural orbitals into the active space was guided by the natural orbital occupation numbers. Thirdly, geometry optimizations with fixed internal coordinate (either τ, α, or α') were performed using the unrestricted natural orbital-complete active space (UNO-CAS) method[60] and the cc-pVDZ basis set. The valence active space for the calculation of the torsional potential of allene consisted of two sets of degenerate π/π^* valence orbitals (0 0 2 2) in terms of $D_2(a\ b_1\ b_2\ b_3)$. For 1,3-difluoroallene analogous molecular orbitals were included in the active space: (2 2) in terms of $C_2(a\ b)$, (1 1 2 0) in terms of $C_{2v}(a_1\ a_2\ b_1\ b_2)$, (0 1 2 1) in terms of $C_{2h}(a_g\ b_g\ a_u\ b_u)$, and (1 3) in terms of $C_s(a'\ a'')$. For both molecules four electrons were set active. Fourthly, the geometries obtained with UNO-CAS(4,4)/cc-pVDZ were further optimized using CASSCF(4,4)/cc-pVTZ calculations. The final geometries along the torsional coordinate for allene that were obtained within the constraints of D_2 symmetry for structures with $0° < \tau < 90°$ and within D_{2h} (D_{2d}) for the structure with $\tau = 0°(90°)$ as well as the final geometries along the torsional coordinate for 1,3-difluoroallene that were obtained within the constraints of C_2 symmetry for structures with $0° < \tau < 180°$ and within C_{2v} (C_{2h}) for the structure with $\tau = 0°(180°)$ were used in subsequent calculations of parity violation and electronic excited states. Moreover, employing the same general procedure without imposing symmetry constraints, we searched for transition states on the ground-state potential-energy surface and calculated the equilibrium geometry of 1,3-difluoroallene.

Lee and Taylor's[61] T_1 diagnostic was calculated for the collinear orthogonal [minimum structure (MS)] and equilibrium geometry [equilibrium structure (ES)] of 1,3-difluoroallene employing the coupled cluster method with both single and double substitutions from the Hartree–Fock determinant as well as noniterative inclusion of triple excitations [i.e., CCSD(T)].

B. Excited electronic states

All calculations of electronically excited states were performed with the MOLCAS 5.2 quantum-chemical program package.[62] The first two valence-excited singlet states of allene and the lowest triplet and singlet excited states of 1,3-difluoroallene were determined for the collinear optimized geometries (see previous section) along the torsional coordinate using the CASSCF method and a small atomic natural orbital ANO-S(4s3p1d/2s) basis set. In the MOLCAS program the D_{2h} point group and its sub-

groups are supported. Thus, all geometries along the torsional coordinate of allene were treated in D_2. The basic valence active space as introduced in the previous section was used. Electronic ground-state energies for the optimized geometries along the torsional coordinate were calculated for allene and 1,3-difluoroallene also using CASSCF(4,4)/ANO-S(4s3p1d/2s), such that relative energies could be determined for the excited-state potential-energy surfaces.

In general a quantitative calculation of the vertical spectrum of a molecule necessitates the inclusion of dynamic electron correlation and a balanced treatment of valence and Rydberg excited states. Here, the complete active space second-order perturbation-theory (CASPT2) method, which is known to account reasonably for a part of the dynamic electron correlation,[63–65] was used. For allene, it has been reported that even the lowest excited states that are of $\pi \rightarrow \pi^*$ character have partially Rydberg-type character and that Rydberg states may appear as low as some of the lowest valence states.[66,67] As Rydberg orbitals are not localized to atoms in the same sense as valence orbitals are, but can rather be considered to be spread out over the entire molecule, for a quantitative calculation of the vertical excitation energies the proper inclusion of diffuse basis functions in the basis set is a prerequisite, such that the $3s$, $3p$, and $3d$ Rydberg states obtained by excitations out of the highest-occupied molecular orbital (HOMO) can be treated in an adequate way. Here, generally contracted basis functions based on atomic natural orbitals[68] (ANOs) were used to construct the molecular orbitals. The contraction scheme used in the calculations was C[4s3p1d]/H[2s], which has been shown to represent an optimal compromise between the quality and size of the corresponding calculation.[65] Single-center diffuse functions were generated using a recently developed procedure to obtain optimal Rydberg basis functions for a given system.[69] The procedure is based on the universal Gaussian basis sets developed by Kaufmann et al.[70] for representing Rydberg and continuum wave functions and has led to augmented ANO basis sets that have been used with success in the calculation of vertical spectra for molecules such as benzene, phenol, and formaldehyde.[69,71] The contraction coefficients for the new Rydberg basis functions are obtained using the procedure of Roos et al.[65] the original ANO-S(4s3p1d/2s) was supplemented with a $1s1p1d$ set of Rydberg functions (contracted from a set of $8s8p8d$ primitives) which were placed at the position of the central C atom of allene. The universal exponents were calculated using the equation

$$\alpha(n,l) = \frac{1}{4n^2(a_l n + b_l)^2}, \tag{2}$$

with the parameters $a_l = 0.584\,342$ $(l=1)$, $0.452\,615$ $(l=2)$, and $0.382\,362$ $(l=3)$ and $b_l = 0.424\,483$ $(l=1)$, $0.309\,805$ $(l=2)$, and $0.251\,333$ $(l=3)$.[70]

The lowest Rydberg state corresponds to the excitation HOMO $\rightarrow 3s$. Further Rydberg states are due to excitations to $3p_x$, $3p_y$, and $3p_z$, and the five components of $3d$. The Rydberg orbitals follow the point-group species arising from their corresponding atomic orbitals. Therefore, in D_2 the $3s$,

$3d_{z^2}$, and $3d_{x^2-y^2}$ Rydberg orbitals belong to the symmetry species a, $3p_z$, and $3d_{xy}$ to b_1, $3p_y$ and $3d_{xz}$ to b_2, and $3p_x$ and $3d_{yz}$ to b_3. These nine lowest Rydberg orbitals classify to (3 2 2 2) in terms of D_2. The final active space employed in our calculations of the vertical excitation energies consists of 13 orbitals, that is $(0\ 0\ 2\ 2)+(3\ 2\ 2\ 2)=(3\ 2\ 4\ 4)$. For each symmetry label of D_2, a state-averaged CASSCF(4,13) calculation was performed and the resulting CASSCF state function was used as a root function of subsequent CASPT2 calculations of the vertical excitation energies for the lowest singlet excited electronic states.

C. Calculations on parity violation

Parity-violating energies were calculated using the multiconfiguration linear-response (MC-LR) approach[10] to electroweak quantum chemistry as implemented in our local version[10] of the DALTON program.[72] Here we just give a brief overview of the general theoretical basis underlying these parity-violation calculations. A more detailed description with further references is provided in Refs. 8–10 and 73. In the absence of external fields and within semirelativistic theory, the leading term of the molecular parity-violating Hamiltonian, representing electron-nucleus interactions and neglecting the nuclear spin-dependent terms, is given in Refs. 7, 9, 10, and 74–76 by an expression that sums over all electrons n and nuclei N of the molecule [here in Système International d'Unités (SI) units][28]

$$\hat{H}_{pv} \approx \frac{\pi G_F}{m_c ch\sqrt{2}}\sum_{i=1}^{n}\sum_{A=1}^{N} Q_w(A)\{\hat{\mathbf{p}}_i \cdot \hat{\mathbf{s}}_i, \delta^3(\mathbf{r}_i-\mathbf{r}_A)\}_+, \quad (3)$$

where Fermi's coupling constant[77] is $G_F=2.222\,527 \times 10^{-14} E_h(a_0)^3$, E_h the Hartree energy, a_0 the Bohr radius, m_e the mass of the electron, c the velocity of light, h Planck's constant, $\hat{\mathbf{p}}_i$ the linear momentum operator of electron i and $\hat{\mathbf{s}}_i$ its spin operator, $\delta^3(\mathbf{r}_i-\mathbf{r}_a)$ the three-dimensional Dirac delta distribution, $\mathbf{r}_j$ the position vector of particle j, $\{\ldots\}_+$ the anticommutator, and $Q_w(A)$ the electroweak charge of nucleus A given by

$$Q_w(A) \approx Z_A(1-4\sin^2\theta_w) - N_A, \quad (4)$$

with Z_A the number of protons and N_A the number of neutrons of nucleus A, and θ_w the Weinberg angle with $\sin^2\theta_w \approx 0.2319$. A more recent value for the weak-mixing angle parameter that is now recommended by the Particle Data Group is $\sin^2\theta_w \approx 0.231\,20(15)$ (see Refs. 77 and 78). The prefactor of $\hat{H}_{pv}$ in Eq. (3), which includes the very small Fermi coupling constant G_F, renders the parity-violating potentials small. Each term in the sum is proportional to the electroweak charge of nucleus A, the value of the electroweak charge in turn being primarily dependent on the number of neutrons of nucleus A, evidencing the predominant role of the neutron-electron interaction. $\hat{H}_{pv}$ transforms odd under space inversion (parity), as it contains the inner product of the linear momentum and spin vector operators. It also contains the three-dimensional Dirac delta distribution because the short-range neutral weak force mediated by the Z^0 boson is essentially a contactlike interaction.[9]

Since $\hat{H}_{pv}$ is a one-electron triplet operator, the expectation value for a nondegenerate singlet eigenstate of a purely electrostatic Hamiltonian would be zero in the nonrelativistic limit.[9,10,79] Thus, spin-orbit coupling corrections to the molecular wave function play an essential role in obtaining nonvanishing parity-violating energies,[80] with the spin-orbit (SO) operator in Breit–Pauli form[81] (here in SI units)

$$\hat{H}_{SO} = \frac{e^2\mu_0}{8\pi m_e^2}\left[\sum_{i=1}^{n}\sum_{A=1}^{N} Z_A\frac{\hat{\mathbf{l}}_{i,A}\cdot\hat{\mathbf{s}}_i}{|\mathbf{r}_A-\mathbf{r}_i|^3} - \sum_{i=1}^{n}\sum_{i\neq j}^{n}\frac{\hat{\mathbf{l}}_{i,j}(\hat{\mathbf{s}}_i+2\hat{\mathbf{s}}_j)}{|\mathbf{r}_i-\mathbf{r}_j|^3}\right], \quad (5)$$

where $\hat{\mathbf{l}}_{i,k}$ is the orbital angular momentum of electron i with respect to the position of particle k and μ_0 is the permeability of the vacuum.[77]

In second-order perturbation theory this spin-orbit coupling gives rise to a nonvanishing parity-violating potential according to[7–10,82]

$$E_{pv} = 2\,\mathrm{Re}\left(\sum_{i\neq 0}\frac{\langle\Psi_0|\hat{H}_{pv}|\Psi_i\rangle\langle\Psi_i|\hat{H}_{SO}|\Psi_0\rangle}{E_0-E_i}\right), \quad (6)$$

where $|\Psi_0\rangle$ denotes the reference state of interest with energy E_0 (usually the singlet ground state) and $|\Psi_i\rangle$ the ith excited (triplet) state with energy E_i. This sum-over-states expression has previously been employed in the single determinant excitation restricted Hartree–Fock[7] (SDE-RHF) and configuration interaction singles excitation restricted Hartree–Fock[8,9] (CIS-RHF) methods. While the latter approach improved the description of the excited states and led to the important theoretical finding of parity-violating energies that were typically one to two orders of magnitude larger than the ones obtained with SDE-RHF, it suffers from the inherent convergence problem associated with the sum-over-states approach. The recent multiconfiguration linear-response (MC-LR) approach[10] that was used in the present work circumvents the convergence problems and improves significantly the description of the reference state. Within the framework of response theory, the parity-violating potential is given by the response of $\langle\Psi_0|\hat{H}_{pv}|\Psi_0\rangle$ to the static (i.e., $\omega=0$) perturbation $\hat{H}_{SO}$ [or equivalently by the response of $\langle\Psi_0|\hat{H}_{SO}|\Psi_0\rangle$ to the static (i.e., $\omega=0$) perturbation $\hat{H}_{pv}$]

$$E_{pv} = \langle\langle\hat{H}_{pv};\hat{H}_{SO}\rangle\rangle_{\omega=0} = \langle\langle\hat{H}_{SO};\hat{H}_{pv}\rangle\rangle_{\omega=0}. \quad (7)$$

It is well known in the framework of propagator methods[83,84] that the expression in Eq. (7) is equivalent to the sum-over-states expression (6) but it can be calculated in a more direct fashion.[10]

The twisting of allenic species similar to ethylene poses particularly for large twisting (i.e., dihedral) angles a multireference problem that requires the use of an appropriate multireference method.[10] The MC-LR approach allows the treatment of such problems by using the CASSCF-LR method.[10] We calculated the parity-violating energies of allene and 1,3-difluoroallene for the aforementioned optimized geometries from $\tau=0°-180°$ in 10° steps using CASSCF-LR(4,4)/cc-pVTZ. Additionally, we calculated for the (C–C–C) collinear orthogonal and the equilibrium structure of

1,3-difluoroallene, both of which are dominated by a single configuration and exhibit small T_1 values, the parity-violating energy differences using the random-phase approximation (RPA) and the Slater-type orbitals with a linear combination of three Gaussian (STO-3G), cc-pVDZ, augmented correlation consistent polarized valence double zeta (aug-cc-pVDZ), and cc-pVTZ basis sets.

III. THEORETICAL RESULTS AND DISCUSSION

A. Ground and electronically excited states of allene and 1,3-difluoroallene

Allene has been the subject of numerous experimental and theoretical investigations. We are particularly interested in its potential-energy surfaces of the ground and excited states along the torsional coordinate, including its barrier heights to internal rotation and its electronic absorption spectrum. The electronic spectrum of allene was measured by Sutcliffe and Walsh[85] and later again in the range from 4.78 to 10.7 eV.[86–88] These studies demonstrated that the absorption spectrum of allene is complex. Below 6.45 eV one finds only a weak structureless absorption. Computationally, the excited states of allene were previously investigated up to about 11 eV using various levels of theory, including the configuration interaction (CI),[66,89,90] equations of motion,[56,57] multireference configuration interaction (MRCI),[56] complete active space self-consistent field (CASSCF),[56] multiconfiguration half-projected Hartree–Fock (MCHPHF),[91] and improved virtual orbital complete active space configuration interaction (IVO-CASCI) method.[92] Computational studies have also dealt with the electronic ground state of allene, particularly the internal (i.e., torsional) rotation of this simple cumulene, including the determination of transition states and corresponding barrier heights to internal rotation.[47–57] At various levels of theory the calculated barrier to internal rotation is predicted to be in the $180-210$ kJ mol^{-1} range. High-level *ab initio* studies predict the corresponding transition structure to be a planar bent C_{2v} symmetric species corresponding to a singlet biradical.[55,56]

The primary aim of our study of the internal rotation of allene was to establish whether the CASSCF method with a small (4,4) CAS would be adequate to reproduce the known essential characteristics of the potential-energy surfaces of the ground and two lowest excited electronic states upon torsional rotation. The motivation for this was threefold: (1) to ensure that CASSCF-LR(4,4) calculations would provide an adequate basis for the calculation of parity-violating energies in allene, using the MC-LR approach as implemented in the DALTON program with CASSCF calculations, (2) to provide a test for our computational investigations of 1,3-difluoroallene, and (3) to provide a basis for the first CASPT2 calculations of allene's vertical excitation spectrum using our newly developed single-center ANO-S Rydberg basis.

Figure 3 shows one-dimensional cuts through the potential-energy surfaces of the electronic ground and two lowest valence-excited singlet states of allene upon CH$_2$ twisting, while the linearity of the CCC chain is maintained. The electronic ground state $^1A_1$ (D_{2d}) correlates with

FIG. 3. Potential-energy surfaces V of the electronic ground state (solid squares) and the two lowest-lying valence-excited singlet states (open squares and circles) of allene as function of the torsional coordinate τ. The former was calculated using CASSCF(4,4)/ANO-S($4s3p1d/2s$), whereas the latter two were calculated using state-averaged CASSCF(4,4)/ANO-S($4s3p1d/2s$) with both states weighted equally.

^1A (D_2) and ^1A_u (D_{2h}). Upon internal rotation the wave function changes its character from a closed-shell singlet to an open-shell singlet. The first excited electronic state $^1A_2$ (D_{2d}) that correlates with ^1B (D_2) and $^1B_{1g}$ (D_{2h}) exhibits energies that remain at about 650 kJ/mol. The second excited state $^1B_1$ (D_{2d}) that correlates with 2^1A (D_2) and ^1A_g (D_{2h}) gets stabilized along the torsional coordinate towards the planar D_{2h} symmetric geometry according to Walsh's rules.[93] At the planar D_{2h} symmetric geometry, the closed-shell ^1A_g state of the second excited electronic state lies 144.5 kJ/mol above the open-shell ^1A_u state. These results indicate that the CASSCF method with a small (4,4) CAS is adequate for our exploratory study and accordingly was used as a basis for our calculations. Our CASPT2 results for the excitation energies are (in eV) 5.96 $(^1A_2)$, 6.48 $(^1B_1)$, 7.07 (^1E), and 7.69 $(^1B_2)$. This compares well with the literature values cited in Table I.

While allene in its equilibrium geometry is D_{2d} symmetric and thus achiral, 1,3-difluoroallene in its equilibrium geometry is predicted to be C_2 symmetric and thus chiral. 1,3-difluoroallene is anticipated to exist in the form of two enantiomers P and M (see Fig. 2). Ogata and Ando[94] calculated a molecular structure for 1,3-difluoroallene using the rotational constants that were obtained using microwave spectroscopy.[41] However, although the experimental data are insufficient for a complete structure determination, they did not report which of the structural parameters were taken as fixed. They probably assumed that the C_2-symmetric 1,3-difluoroallene exhibits a collinear C=C=C moiety. Thus, its geometry is experimentally not precisely known.

Table II summarizes the structural parameters of the equilibrium structure that we obtained in comparison to previously reported experimental as well as theoretical data (see also the structure ES shown in Fig.5). All calculations predict that 1,3-difluoroallene deviates from CCC collinearity. The occurrence and extent of such nonclassical distortions at multiple bonds is, in a simple valence bond modeling, related to the singlet-triplet separation of the interacting fragments forming the multiple bond, and have previously been suggested for substituted allenes.[95] In fact, a $1.8° \pm 0.6°$ deviation from collinearity was found experimentally for the related molecule fluoroallene (CH$_2$=C=CHF).[96] Because

TABLE I. Overview of experimental and theoretical excitation energies of allene. All energies are given in (eV).

State	$1\,^1A_2$	$1\,^1B_1$	$1\,^1E$	$1\,^1B_2$
Experimental data[a]	<6.45[b]	⋯	6.5–6.9	6.95–7.85
			(6.70 max)[b]	(7.23 max)[b]
			6.5–6.9	7.1–7.5
			(6.71 max)[c]	(7.27 max)[c]
CASPT2 (this work)	5.96	6.48	7.07	7.69
IVO-CASCI[d]	6.60	7.16	7.38	8.03
CASSCF(8,10)/ANO(2+)[e]	5.89	6.55	6.84	7.13
MRCI(4,8)/ANO(2+)[e]	6.19	6.70	6.85	7.55
MRCI+D/ANO(2+)[e]	6.10	6.55	6.94	7.56
EOM-CCSD/6-311++G**[e]	6.23	6.65	7.02	7.62
CI[f]	6.92	7.45	7.56	⋯
CI[g]	6.566	6.921	6.872	7.445
EOM/6-31G**[h]	7.76	7.32	⋯	9.70
EOM/6-31G**+Rydberg[h]	6.86	7.23	7.73	8.03
CI[i]	6.49	6.84	7.21	7.88

[a]Assignment of Diamond and Segal (see Ref. 90).
[b]Optical-absorption (obsd) data from Rabalais *et al.* (see Ref. 86).
[c]Magnetic circular dichroism data (obsd) from Fukc and Schnepp (see Ref. 88).
[d]Reference 92.
[e]Reference 56.
[f]Reference 89.
[g]Reference 90.
[h]Reference 67.
[i]Reference 66.

the experimental geometry was not determined precisely, a comparison with theoretically calculated geometries is limited. Moreover, even for fluoroallene and 1,1-difluoroallene ($CH_2{=}C{=}CF_2$) where five isotopic species were studied using microwave spectroscopy,[96,97] the experimental uncertainties in some of the structural parameters are comparably large. This limits conclusions that can be drawn about 1,3-difluoroallene by comparison with those molecules.

Our CASSCF results agree well with the experimentally reported structure, albeit they highlight that theory predicts 1,3-difluoroallene to deviate from CCC collinearity in its C_2-symmetric equilibrium geometry. The structural parameters of 1,3-difluoroallene's equilibrium geometry (see structure ES in Fig. 5) and those of its collinear and orthogonal ($\tau{=}90°$) geometry (see structure MS in Fig. 5) are very

TABLE III. Energies E of the transition structures (TS1-3) of 1,3-difluoroallene, the C_2-symmetric minimum structure (MS), the C_2-symmetric equilibrium structure (ES), and their relative energies with respect to ES, calculated using CASSCF(4,4)/cc-pVTZ. ZPC: with zero-point energy correction.

Structure	E/E_h	E_{ZPC}/E_h	$E_{rel}/(kJ/mol)$	$E_{ZPC,rel}/(kJ/mol)$
ES	−313.722 079 4	−313.679 350	0	0
MS	−313.721 969 7	−313.679 417	0.288 017 35	−0.175 908 5
TS1	−313.649 422 7	−313.609 440	190.760 165 8	183.548 705
TS2	−313.651 795 6	−313.609 037	184.530 116 9	184.606 781 5
TS3	−313.646 616 5	−313.603 631	198.127 843 9	198.800 234 5

similar. Thus, a deviation from collinearity and a corresponding change in dihedral angle have a negligible effect on the size of the remaining structural parameters. The CCC collinear structure is only about 0.3 kJ mol^{-1} (25 cm^{-1}) higher in energy than the equilibrium geometry (see Table III). This is much less than the zero-point energy, indicating a dynamically quasicollinear structure of the CCC frame. Anyway, 25 cm^{-1} is presumably not physically relevant within the numerical precision of these calculations. This is also supported by a formal zero-point energy correction, which renders the collinear structure lowest in energy. The two enantiomers of 1,3-difluoroallene can be interconverted by internal rotation along the torsional coordinate. A single transition state is found for the internal rotation of allene, which is a planar bent C_{2v}-symmetric species corresponding to a $^1A_2$ singlet biradical. However, one finds three transition states in the case of 1,3-difluoroallene, which is of lower symmetry.

Along the torsional coordinate the potential energy increases (middle part of Fig. 4) and reaches a maximum at the planar C_{2v} and C_{2h} symmetric geometries. Starting from these planar geometries, the barriers to stereomutation decrease initially with in-plane CCC bending (upper left and right) and increase with out-of-plane CCC bending (lower left and right). This behavior is analogous to what has been reported in the literature for allene (see, for example, Refs. 55–57), but leads in the case of 1,3-difluoroallene to three transition structures with different symmetries and energies. The nature of each structure as belonging to a transition state was confirmed by harmonic frequency calculations, where

TABLE II. Structural parameters of the experimental and *ab initio* calculated equilibrium geometry of 1,3-difluoroallene. Uncorrected values are given.

Parameter	Expt.[a]	SCF/DZ+D$_c$ (Ref. 43)	DFT(B3PW91)/ aug-cc-pVTZ (Ref. 45)	CASSCF(4,4)/cc-pVTZ, this work
$r(C{=}C)/Å$	1.306	1.296	1.298	1.306
$r(C{-}F)/Å$	1.330	1.334	1.343	1.322
$r(C{-}H)/Å$	1.086	1.074	1.084	1.070
α (FCC)/°	124.2	122.6	122.72	122.0
α (FCH)/°	114.7	112.4	112.16	113.2
α (CCC)/°	180 (fixed?)[a]	178.9	175.75	170.7
τ/°	92	90 (fixed?)[b]	91.7	93.1

[a]Determined from 1,3-difluoroallene's rotational constants (Ref. 39) using unreported assumptions for some of the structural parameters (see Ref. 94).
[b]The dihedral angle is neither given nor derivable from the data given by Dixon and Smart (see Ref. 43). However, it appears likely that they had fixed it to 90° during the geometry optimization.
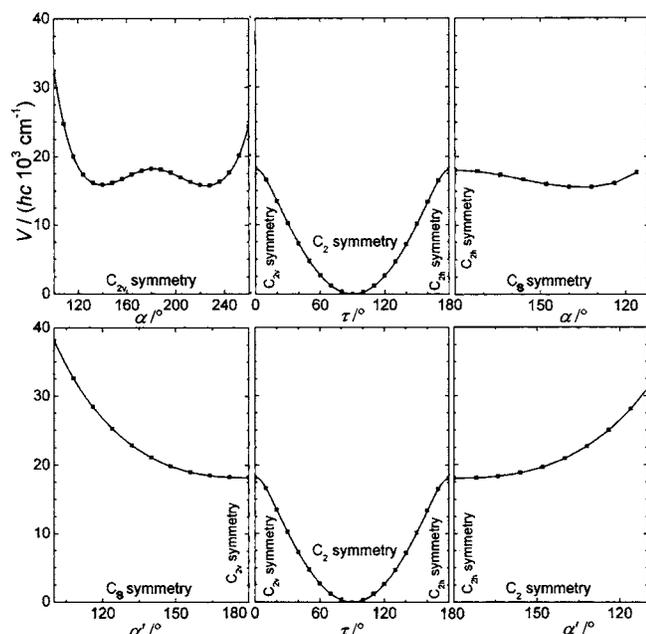
FIG. 4. Ground-state potential-energy surface of 1,3-difluoroallene, calculated along the torsional τ, the in-plane α and out-of-plane α' CCC-bending coordinates using CASSCF(4,4)/cc-pVTZ.

FIG. 5. Characteristic structures on the electronic ground-state potential-energy surface. All bond lengths are given in angstroms. Upper left: C_2-symmetric minimum structure (MS); upper right: C_2-bent symmetric equilibrium structure (ES), left center: C_{2v}-symmetric transition structure (TS1); lower left: C_1-symmetric transition structure (TS2); lower right: C_s-symmetric transition structure (TS3). All structures were obtained in CASSCF(4,4)/cc-pVTZ geometry optimizations.

one imaginary frequency was obtained for each structure. Absolute energies for these transition structures as well as their energies with respect to the C_2-symmetric equilibrium structure are given in Table III. Accordingly, the barrier heights to stereomutation between the two enantiomers of 1,3-difluoroallene lie between 184 and 198 kJ mol^{-1} (similar to barriers predicted for allene, 180–210 kJ mol^{-1}, and experimental barrier heights of 1,3-dimethylallene and 1,3-di-*tert*-butylallene as determined to date by Roth *et al.*,[98] 193.3 kJ mol^{-1} for the former allene derivative and 196.2 kJ mol^{-1} for the latter). Future calculations that would take more dynamic electron correlation into account might yield somewhat smaller barrier heights.

It is particularly noteworthy that the chiral C_1 asymmetric transition state TS2 (see Fig. 5) is lowest in electronic energy, while with zero-point corrections the C_{2v} symmetric TS1 becomes lowest. However, the differences are too small to be significant and the transition states should be considered as part of a set of "nonrigid transition states."[99]

Figure 6 shows our results for the potential-energy surfaces (PES) of the electronic ground state and the lowest valence-excited singlet states, calculated using CASSCF(4,4)/ANO-S(4s3p1d/2s). As has also been reported for allene, the ground-state PES of 1,3-difluoroallene is dominated by a closed-shell configuration in the orthogonal geometries and by an open-shell configuration in the planar geometries. The lowest electronically excited state is predicted to be the ^3A state. The first singlet excited state is the valence-excited state ^1A. The corresponding vertical excitation energies are predicted at 4.59 and 6.95 eV, respectively. The potential-energy surfaces of excited states along the torsional coordinate were calculated at the geometries that were optimized in the electronic ground state and exhibit minima at the planar geometries suggesting that 1,3-difluoroallene may be a chiral molecule with achiral excited states. Such a

characteristic is of great interest for proposed experiments that aim to measure directly the parity-violating energy difference or to achieve coherently controlled asymmetric synthesis using linearly polarized light.[100] Even if the minimum geometries in the excited states were slightly distorted and even chiral, they are expected to exhibit low barriers to a coplanar achiral structure and thus rovibrational states of well-defined parity at moderate excitations. From a formal point of view, it is conceivable that 1,3-difluoroallene enantiomerizes along a completely chiral path, similar to other cases that have been discussed following the early sugges-
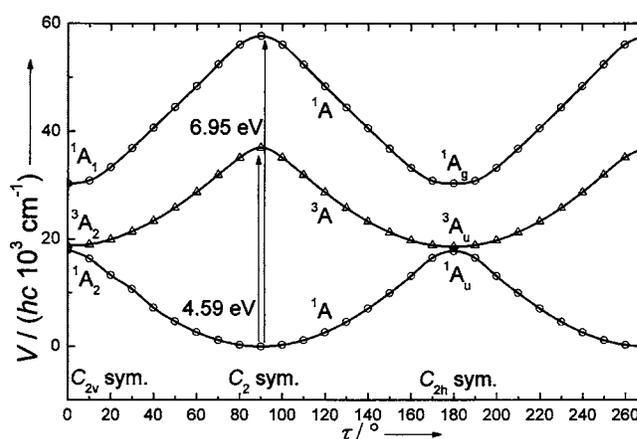
FIG. 6. Potential-energy surfaces V of the electronic ground state (lower curve) and the two lowest valence-excited states (open triangles and circles) of 1,3-difluoroallene as function of the torsional coordinate τ. All energies were calculated using CASSCF(4,4)/ANO-S(4s3p1d/2s).
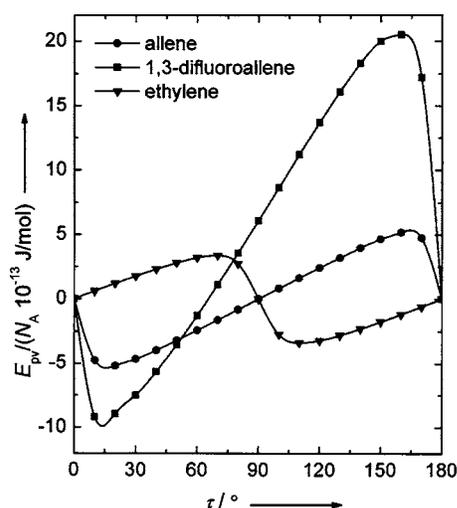
FIG. 7. Parity-violating potentials for allene (circles) and 1,3-difluoroallene (squares; the range of the dihedral angle from 0° to 180° corresponds to the P enantiomer of 1,3-difluoroallene) along the torsional coordinate τ that were calculated using CASSCF-LR(4,4)/cc-pVTZ. The parity-violating potentials are compared to those of ethylene (triangles) that were calculated using a full-valence CASSCF-LR/TZ** calculation (see Ref. 10).

tion of Mislow,[101] and rather special compounds investigated by Mauksch and Schleyer[102] or even chirally substituted methane CHDTMu.[103,104] However, this statement has little physical significance in view of the highly nonrigid transition structures, which may interconvert easily and thus we have not pursued these geometrical details any further.

B. Parity violation in allene, 1,3-dideuteroallene and 1,3-difluoroallene

Figure 7 shows the parity-violating potentials $E_{pv}(\tau)$ for allene and 1,3-difluoroallene in comparison to the one of ethylene[10] as calculated at the CASSCF-LR level of theory. All potentials show the typical dependence on the dihedral angle with large excursions from negative to positive values and zero crossing at a chiral geometry for 1,3-difluoroallene, as was also found for other torsional parity-violating potentials (see Refs. 8–10, 30, 32, and 33 and references cited therein). Allene and ethylene are achiral in their equilibrium geometries and exhibit achiral transition structures. Thus, the parity-violating energies vanish also by symmetry for the corresponding structures. All other structures are chiral and accordingly can exhibit parity-violating energies. $E_{pv}(\tau)$ has a similar form for allene and ethylene and is antisymmetric with respect to the point at $\tau=90°$. However, the parity-violating potential of allene is shifted along the torsional coordinate by 90°, because allene has its equilibrium geometry at $\tau=90°$, whereas for ethylene it is at $\tau=0°$. The maximum value of $E_{pv}(\tau)$ in allene is slightly (about 1.5 times) larger than for ethylene. $E_{pv}(\tau)$ for 1,3-difluoroallene shows in comparison to allene three essential differences. Firstly, the maximum value of $E_{pv}(\tau)$ is about four times larger than the one for allene. Secondly, the parity-violating potential of 1,3-difluoroallene is not antisymmetric with respect to the point at $\tau=90°$, because 1,3-difluoroallene is chiral in its equilibrium geometry and thus $E_{pv}(\tau)$ does not vanish at $\tau=90°$. The M enantiomer (see Fig. 2) is calculated to be

TABLE IV. Parity-violating energy difference $\Delta_{pv}E=E_{pv}(P)-E_{pv}(M)$ for the collinear orthogonal (MS) and the equilibrium structure (ES) of 1,3-difluoroallene calculated with different basis sets and the MC-LR approach to electroweak quantum chemistry.

Method	Structure	$\Delta_{pv}E/(hc10^{-13}\,cm^{-1})$
RPA/STO-3G	MS	0.36
	ES	0.31
RPA/cc-pVDZ	MS	1.05
	ES	0.92
RPA/aug-cc-pVDZ	MS	1.02
	ES	0.89
RPA/cc-pVTZ	MS	1.29
	ES	1.12
CASSCF-LR(4,4)/cc-pVTZ	MS	1.02

stabilized compared with the P enantiomer. As mentioned in the previous section, 1,3-difluoroallene is dominated by a closed-shell configuration in the collinear orthogonal geometry (MS). To obtain additional insight into the question of the quality of the HF single determinant as reference for possible single-reference calculations, we calculated Lee and Taylor's T_1 diagnostic, usually a byproduct when employing CCSD(T)/cc-pVTZ.[61] We obtained a T_1 value of about 0.0136. For $T_1<0.02$ the wave function may be assumed to have significant single-determinant character, and accordingly the HF single determinant should be well suited as reference in a single-reference calculation. Thus, parity-violating calculations using the MC-LR approach to electroweak quantum chemistry in the random-phase approximation should lead to good results for 1,3-difluoroallene in its collinear orthogonal (MS) as well as in its equilibrium structure (ES). Table IV summarizes our results for the parity-violating energy differences of 1,3-difluoroallene. Calculated parity-violating energy differences for the collinear structure are about 15% larger than the ones for the equilibrium geometry. The results obtained at our lowest level of theory, that is RPA with the minimum basis set STO-3G, are only about a factor of 3 smaller than the one obtained at our highest level of theory, that is, CASSCF-LR(4,4) with a correlation consistent cc-pVTZ basis set. For the cc-pVTZ basis set, RPA yields parity-violating energy differences that compare well with the ones that were obtained with the CASSCF-LR multiconfiguration method, the small (∼20%) differences being indicative of the size of correlation effects. Overall, we predict at all levels of theory that the M enantiomer of 1,3-difluoroallene is stabilized compared with the P enantiomer by about $N_A\Delta_{pv}E^{el}\approx 1.2 \times 10^{-12}$ J mol^{-1}. Given the nonrigidity of the vibrational ground state of difluoroallene, there may be sizable corrections due to zero-point averaging, which would have to be added to these purely electronic values.[28] However, these will not change the order of magnitude and are not expected to be larger than the remaining uncertainties resulting from the limited convergence of the electronic structure calculations at this stage. The relativistic corrections are certainly small for this molecule. Thus, while for very high accuracy of the calculations in a possible future analysis of experiments, in particular, electron correlation and vibrational ef-

fects must be taken into account, these will not change the conclusions of the present paper aiming at an exploratory study preparing for such experiments.

Allene can also be rendered chiral by 1,3-deuteration. However, in the framework of the Born–Oppenheimer approximation, all nuclei for which the electronic wave function remains invariant under improper rotations S_n do not contribute to the parity-violating energy.[105] Thus, for symmetry reasons, 1,3-deuteration of D_{2d}-symmetric allene leading to C_2 symmetric and chiral 1,3-dideuteroallene is not expected to lead to appreciable electronic parity-violating energy differences. In fact, for any isotopically substituted D_{2d}-symmetric allene the purely electronic parity-violating energy differences should be zero. Nonzero parity-violating energy differences are likely to arise due to zero-point averaging. However, one may safely assume that the final $\Delta_{pv}E$ for dideuteroallene will be smaller than for difluoroallene (see also Refs. 25 and 107).

IV. CONCLUSIONS AND OUTLOOK

The present paper reports the first calculations of parity-violating potentials as a function of torsional angle in allene and 1,3-difluoroallene, the latter being chiral in its equilibrium geometry. From these calculations as well as from the ordinary, parity-conserving quantum-chemical energies we can draw the following main conclusions:

(i)   Allene shows maximum parity-violating potentials at chiral geometries of rather similar magnitude as ethylene,[10] on the order of 0.5 pJ mol^{-1} ($\simeq 4 \times 10^{-14}$ cm^{-1}), with a zero value at the achiral equilibrium geometry with torsional angle $\tau = 90°$ (see Fig. 7).

(ii)   In 1,3-difluoroallene the structure is chiral at $\tau = 90°$ and thus the parity-violating potential at the equilibrium geometry is nonzero giving rise to a parity-violating energy difference between enantiomers $\Delta_{pv}E = E_{pv}(P) - E_{pv}(M) = 1.2$ pJ mol^{-1} (1×10^{-13} cm^{-1}) at the highest levels of theory employed here. Remaining uncertainties arise mainly from the limited basis set size, the omission of vibrational averaging, and smaller relativistic effects and can be estimated to be within less than a factor of 2 altogether. The corresponding period for parity change is 333 s (the "parity-violating time" τ_{pv}).

(iii) The qualitative behavior of the parity-violating potential in 1,3-difluoroallene as a function of the torsional angle τ is interestingly similar to the one in allene, but asymmetrically shifted from $\tau = 90°$ with a larger maximum value of 2 pJ mol^{-1} near $\tau = 150°$ and a minimum of -1 pJ mol^{-1} near $\tau = 15°$ (see Fig. 7).

(iv)   Calculations on the barrier heights for internal rotation provide a first result of $184-198$ kJ mol^{-1} for the stereomutation barrier in 1,3-difluoroallene, fairly similar to an experimental result for 1,3-dimethylallene[98] (193 kJ mol^{-1}). Independent of the precise accuracy of these barrier heights, one can therefore estimate the stereomutation tunneling splittings for the hypothetical symmetrical case to be sev-
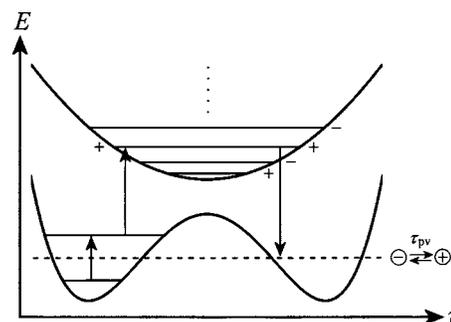
FIG. 8. Schematic diagram for rovibrational state and parity selection using an achiral planar or quasiplanar intermediate excited state of a molecule which is chiral in the ground state (see also Refs. 6 and 25) and paper II (Ref. 46). The real-potential surface is multidimensional and the preexcitation may occur in a mode different but coupled to the torsional mode.

eral ten orders of magnitude smaller than $\Delta_{pv}E$ [from very rough WKB estimates and by comparison with S$_2$Cl$_2$ (Ref. 106) and ^{1,2,3}H$_2$X$_2$, X=O, S, Se, Te,[30,32,33] which all have much lower barriers to stereomutation]. Thus, 1,3-difluoroallene is a chiral molecule where parity violation dominates over tunneling and $\Delta_{pv}E$ corresponds to a measurable ground-state energy difference of the enantiomers. The transition states for stereomutation in 1,3-difluoroallene are highly nonrigid,[99] with several identified transition structures of fairly similar energy, two of which being chiral (enantiomeric) structures (TS2 in Table III) thus allowing in principle for a completely chiral stereomutation pathway.[101–104]

(v)   Calculations on the low-lying ^3A and ^1A excited states of 1,3-difluoroallene show them to be planar or quasiplanar (nonrigid) structures, fairly similar to the already established situation in allene. This quasiplanar structure allows for the possibility of isolated rovibrational levels of well-defined parity, which is a requirement for realizing the scheme proposed some time ago[18] to directly measure $\Delta_{pv}E$ using an intermediate spectroscopic level of well-defined parity. In the time-dependent variant of this experiment an initial time evolution of a superposition state of well-defined parity in the ground electronic state on the millisecond time scale should be observable spectroscopically, even though $\Delta_{pv}E$ is relatively small for 1,3-difluoroallene.

The necessary rovibrational state selection in such a future experiment will be greatly aided by a two-step (or even three, four, or more step) experiment with infrared preexcitation in the electronic ground state following the scheme in Fig. 8. In this context we report in paper[46] II the first high-resolution rovibrational analysis of the infrared spectrum of 1,3-difluoroallene. In principle, our results are also of relevance for measuring parity violation in 1,3-difluoroallene by rotational[14,22] or vibrational[15,16,24] frequency shifts, but because of the small size of the these effects, experimental technology would currently seem to be insufficient and the superposition approach[18] more promising for this molecule. In any case, the results reported here and in Ref. 46 consti-

tute major steps forward towards experiments on the parity-violating energy differences $\Delta_{pv}E$ in enantiomers of chiral molecules.

ACKNOWLEDGMENTS

[1] T. D. Lee and C. N. Yang, Phys. Rev. **104**, 254 (1956).
[2] C. S. Wu, E. Ambler, R. W. Hayward, D. D. Hoppes, and R. P. Hudson, Phys. Rev. **105**, 1413 (1957).
[3] R. L. Garwin, L. M. Lederman, and M. Weinrich, Phys. Rev. **105**, 1415 (1957).
[4] Y. J. Yamagata, J. Theor. Biol. **11**, 495 (1966).
[5] R. Janoschek, in *Chirality*, edited by R. Janoschek (Springer, Berlin, 1991), pp. 18.
[6] M. Quack, Angew. Chem., Int. Ed. **41**, 4618 (2002).
[7] R. A. Hegstrom, D. W. Rein, and P. G. H. Sandars, J. Chem. Phys. **73**, 2329 (1980).
[8] A. Bakasov, T.-K. Ha, and M. Quack, in *Proceedings of the Fourth Trieste Conference (1995), Chemical Evolution: Physics of the Origin and Evolution of Life*, edited by J. Chela-Flores and F. Rolin (Kluwer Academic, Dordrecht, 1996), pp. 287–296.
[9] A. Bakasov, T.-K. Ha, and M. Quack, J. Chem. Phys. **109**, 7263 (1998); **110**, 6081 (1999).
[10] R. Berger and M. Quack, J. Chem. Phys. **112**, 3148 (2000).
[11] P. Lazzeretti and R. Zanasi, Chem. Phys. Lett. **279**, 349 (1997); **286**, 240 (1998).
[12] J. K. Laerdahl and P. Schwerdtfeger, Phys. Rev. A **60**, 4439 (1999).
[13] A. C. Hennum, T. Helgaker, and W. Klopper, Chem. Phys. Lett. **354**, 274 (2002).
[14] M. Quack and J. Stohner, Phys. Rev. Lett. **84**, 3807 (2000).
[15] V. S. Letokhov, Phys. Lett. A **53**, 275 (1975); O. N. Kompanets, A. R. Kukudzhanov, V. S. Letokhov, and L. L. Gervits, Opt. Commun. **19**, 414 (1976).
[16] E. Arimondo, P. Glorieux, and T. Oka, Opt. Commun. **23**, 369 (1977).
[17] R. A. Harris and L. Stodolski, Phys. Lett. **78**, 313 (1978).
[18] M. Quack, Chem. Phys. Lett. **132**, 147 (1986).
[19] A. L. Barra, J. B. Robert, and L. Wiesenfeld, Phys. Lett. A **115**, 443 (1986).
[20] L. Wiesenfeld, Mol. Phys. **64**, 739 (1988).
[21] J. B. Robert and A. L. Barra, Chirality **13**, 699 (2001).
[22] A. Bauder, A. Beil, D. Luckhaus, F. Müller, and M. Quack, J. Chem. Phys. **106**, 7558 (1997).
[23] C. Daussy, Thèse, Université Paris 13, 1999.
[24] C. Daussy, T. Marrel, A. Amy-Klein, C. T. Nguyen, C. J. Borde, and C. Chardonnet, Phys. Rev. Lett. **83**, 1554 (1999).
[25] M. Quack, Angew. Chem., Int. Ed. Engl. **28**, 571 (1989).
[26] A. Szabo-Nagy and L. Keszthelyi, Proc. Natl. Acad. Sci. U.S.A. **96**, 4252 (1999); L. Keszthelyi, J. Biol. Phys. **20**, 241 (1994).
[27] M. Quack and J. Stohner, Chirality **13**, 745 (2001).
[28] M. Quack and J. Stohner, J. Chem. Phys. **119**, 11228 (2003).
[29] A. S. Lahamer, S. M. Mahurin, R. N. Compton, D. House, J. K. Laerdahl, M. Lein, and P. Schwerdtfeger, Phys. Rev. Lett. **85**, 4470 (2000); J. K. Laerdahl, P. Schwerdtfeger, and H. M. Quiney, *ibid.* **84**, 3811 (2000).
[30] M. Gottselig, D. Luckhaus, M. Quack, J. Stohner, and M. Willeke, Helv. Chim. Acta **84**, 1846 (2001).
[31] M. Quack and M. Willeke, Helv. Chim. Acta **86**, 1641 (2003).
[32] M. Gottselig, M. Quack, and M. Willeke, Isr. J. Chem. **43**, 353 (2003).
[33] M. Gottselig, M. Quack, J. Stohner, and M. Willeke, Int. J. Mass. Spectrom. **233**, 373 (2004).
[34] M. Quack (unpublished) as cited in P. Pfeiffer, in *Energy Storage and Redistribution in Molecules*, Proceedings of Two Workshops, Bielefeld, June 1980, edited by J. Hinze (Plenum, New York, 1983), p. 315; see also M. Quack, in *Femtosecond Chemistry*, edited by J. Manz and L. Woeste
(Wiley VCH, Weinheim, 1994), Chap. 27, Vol. 2, p. 781.
[35] R. A. Harris and L. Stodolski, J. Chem. Phys. **74**, 2145 (1981); A. Cina and R. A. Harris, *ibid.* **100**, 2531 (1994).
[36] R. Marquardt and M. Quack, Z. Phys. D: At., Mol. Clusters **36**, 229 (1996).
[37] P. Kral, I. Thanopulos, M. Shapiro, and D. Cohen, Phys. Rev. Lett. **90**, 033001 (2003).
[38] D. Gerbasi, P. Brumer, I. Thanopulos, P. Kral, and M. Shapiro, J. Chem. Phys. **120**, 11557 (2004).
[39] A. P. Zens, P. D. Ellis, and R. Ditchfield, J. Am. Chem. Soc. **96**, 1309 (1974).
[40] M. J. Bunegar, R. Fields, and R. N. Haszeldine, J. Fluorine Chem. **15**, 497 (1980).
[41] P. D. Ellis, Y. S. Li, C. C. Tong, A. P. Zens, and J. R. Durig, J. Chem. Phys. **62**, 1311 (1975).
[42] J. R. Durig, Y. S. Li, J. D. Witt, A. P. Zens, and P. D. Ellis, Spectrochim. Acta, Part A **33**, 529 (1977).
[43] D. A. Dixon and B. E. Smart, J. Phys. Chem. **93**, 7772 (1989).
[44] I. Novak, J. Org. Chem. **66**, 3600 (2001).
[45] J. E. Rode and J. C. Dobrowolski, J. Mol. Struct.: THEOCHEM **635**, 151 (2003).
[46] S. Albert, M. Gottselig, M. Quack, and J. Stohner (in preparation).
[47] R. J. Buenker, J. Chem. Phys. **48**, 1368 (1968).
[48] L. Radom and J. A. Pople, J. Am. Chem. Soc. **92**, 4786 (1970).
[49] L. J. Schaad, Tetrahedron **26**, 4115 (1970).
[50] V. Staemmler, Theor. Chim. Acta **45**, 89 (1977).
[51] R. Seeger, R. Krishnan, J. A. Pople, and P. v. R. Schleyer, J. Am. Chem. Soc. **99**, 7103 (1977).
[52] C. E. Dykstra, J. Am. Chem. Soc. **99**, 2060 (1977).
[53] S. Xantheas, S. T. Elbert, and K. Ruedenberg, Theor. Chim. Acta **78**, 365 (1991).
[54] P. Valtazanos, S. T. Elbert, S. Xantheas, and K. Ruedenberg, Theor. Chim. Acta **78**, 287 (1991).
[55] H. F. Bettinger, P. R. Schreiner, P. v. R. Schleyer, and H. F. Schaefer III, J. Phys. Chem. **100**, 16147 (1996).
[56] W. M. Jackson, A. M. Mebel, S. H. Lin, and Y. T. Lee, J. Phys. Chem. A **101**, 6638 (1997).
[57] H. F. Bettinger, Dissertation, Erlangen, 1998.
[58] M. J. Frisch, G. W. Trucks, H. B. Schlegel *et al.*, GAUSSIAN 98 (Pittsburgh, PA 15106, U.S.A., 1998).
[59] P. Pulay and T. P. Hamilton, J. Chem. Phys. **88**, 4926 (1988).
[60] J. M. Bofill and P. Pulay, J. Chem. Phys. **90**, 3637 (1989).
[61] T. J. Lee and P. R. Taylor, Int. J. Quantum Chem., Quantum Chem. Symp. **23**, 199 (1989).
[62] K. Andersson, M. Barysz, A. Bernhardsson *et al.*, MOLCAS Version 5.2 (Lund University, Sweden, 2001).
[63] K. Andersson, P. A. Malmqvist, B. O. Roos, A. J. Sadlej, and K. Wolinski, J. Phys. Chem. **94**, 5483 (1990); K. Andersson, P. A. Malmqvist, and B. O. Roos, J. Chem. Phys. **96**, 1218 (1992).
[64] B. O. Roos, Acc. Chem. Res. **32**, 137 (1999).
[65] B. O. Roos, K. Andersson, M. P. Fulscher, P. A. Malmqvist, L. Serrano-Andrés, K. Pierloot, and M. Merchan, Adv. Chem. Phys. **93**, 219 (1996).
[66] A. Rauk, A. F. Drake, and S. F. Mason, J. Am. Chem. Soc. **101**, 2284 (1979).
[67] V. Galasso and G. Fronzoni, J. Mol. Struct.: THEOCHEM **26**, 235 (1985).
[68] P. O. Widmark, P. A. Malmqvist, and B. O. Roos, Theor. Chim. Acta **77**, 291 (1990).
[69] J. Lorentzon, P. A. Malmqvist, M. Fulscher, and B. O. Roos, Theor. Chim. Acta **91**, 91 (1995).
[70] K. Kaufmann, W. Baumeister, and M. Jungen, J. Phys. B **22**, 2223 (1989).
[71] M. Merchan and B. O. Roos, Theor. Chim. Acta **92**, 227 (1995).
[72] T. Helgaker, H. J. Jensen, P. Jørgenson *et al.*, DALTON: An electronic structure program (1997).
[73] A. Bakasov and M. Quack, Chem. Phys. Lett. **303**, 547 (1999).
[74] M. Bouchiat and C. Bouchiat, J. Phys. (Paris) **35**, 899 (1974).
[75] S. Mason and G. Tranter, Mol. Phys. **53**, 1091 (1984).
[76] A. L. Barra, J. B. Robert, and L. Wiesenfeld, Europhys. Lett. **5**, 217 (1988).
[77] E. R. Cohen, T. Cvitas, J. G. Frey *et al.*, *Quantities, Units, and Symbols in Physical Chemistry*, 3rd ed. (to be published).
[78] S. Eidelman, K. G. Hayes, K. A. Olive *et al.*, Phys. Lett. B **592**, 1 (2004).
[79] R. Berger, Phys. Chem. Chem. Phys. **5**, 12 (2003).

[80] E. Gajzago and G. Marx, ATOMKI Kozl. Suppl. **16**, 177 (1974).

[81] G. Breit, Phys. Rev. **34**, 553 (1929); **36**, 383 (1930); **39**, 616 (1932); W. Pauli, Z. Phys. **43**, 601 (1927).

[82] B. Y. Zel'dovich, D. B. Saakyan, and I. I. Sobel'man, Sov. Phys. JETP **25**, 94 (1977).

[83] J. Linderberg and Y. Öhrn, *Propagators in Quantum Chemistry*, 2nd ed. (Wiley, New York, 2004).

[84] F. Jensen, *Introduction to Computational Chemistry* (Wiley, New York, 1999).

[85] L. H. Sutcliffe and A. D. Walsh, J. Chem. Phys. **19**, 1210 (1951); J. Chem. Soc.(Mar), 899 (1952).

[86] J. W. Rabalais, J. M. McDonald, V. Scherr, and S. P. McGlynn, Chem. Rev. (Washington, D.C.) **71**, 73 (1971).

[87] A. A. Iverson and B. R. Russel, Spectrochim. Acta, Part A **28**, 447 (1972).

[88] K. Fuke and O. Schnepp, Chem. Phys. **38**, 211 (1979).

[89] B. Lam and R. P. Johnson, J. Am. Chem. Soc. **105**, 7479 (1983).

[90] J. Diamond and G. A. Segal, J. Am. Chem. Soc. **106**, 952 (1984).

[91] P. Otto and M. B. Ruiz, J. Mol. Struct.: THEOCHEM **433**, 131 (1998).

[92] R. K. Chaudhuri, K. F. Freed, and D. M. Potts, in *Low-Lying Potential Energy Surfaces*, edited by M. R. Hoffman and K. G. Dyall (Oxford University Press, Washington, D.C., 2002), Vol. 828, p. 154.

[93] R. J. Buenker and S. D. Peyerimhoff, Chem. Rev. (Washington, D.C.) **74**, 127 (1974).

[94] T. Ogata and B.-I. Ando, J. Mol. Spectrosc. **118**, 70 (1986).

[95] G. Trinquier and J. P. Malrieu, J. Am. Chem. Soc. **109**, 5303 (1987).

[96] T. Ogata, K. Fujii, M. Yoshikawa, and F. Hirota, J. Am. Chem. Soc. **109**, 7639 (1987).

[97] J. R. Durig, Y. S. Li, C. C. Tong, A. P. Zens, and P. D. Ellis, J. Am. Chem. Soc. **96**, 3805 (1974).

[98] W. R. Roth, G. Ruf, and P. W. Ford, Chem. Ber. **107**, 48 (1974); **107**, 48 (1974).

[99] M. Quack, Faraday Discuss. Chem. Soc. **71**, 309 (1981).

[100] M. Shapiro, E. Frishman, and P. Brumer, Phys. Rev. Lett. **84**, 1669 (2000).

[101] K. Mislow, Science **120**, 232 (1952).

[102] M. Mauksch and P. V. v. R. Schleyer, Angew. Chem., Int. Ed. Engl. **36**, 1856 (1997); P. V. v. R. Schleyer and M. Mauksch, *ibid.* **39**, 2756 (2000).

[103] M. J. M. Pepper, I. Shavitt, P. v. R. Schleyer, M. N. Glukhovtsev, R. Janoschek, and M. Quack, J. Comput. Chem. **16**, 207 (1995).

[104] R. Marquardt and M. Quack, J. Phys. Chem. A **108**, 3166 (2004).

[105] R. Berger, M. Quack, A. Sieben, and M. Willeke, Helv. Chim. Acta **86**, 4048 (2003).

[106] R. Berger, M. Gottselig, M. Quack, and M. Willeke, Angew. Chem., Int. Ed. **40**, 4195 (2001).

[107] R. Berger, G. Laubeudes, M. Quack, A. Sieben, J. Stohner, and M. Willeke, Angew. Chem., Int. Ed. Engl. **44**, 3623 (2005).